Int J Thermophys (2010) 31:1371–1385
DOI 10.1007/s10765-010-0715-y

Dielectric-Constant Gas-Thermometry Measuring System for the Determination of the Boltzmann Constant at PTB

T. Zandt · B. Fellmuth · C. Gaiser · A. Kuhn

Received: 18 November 2009 / Accepted: 23 January 2010 / Published online: 3 March 2010

Abstract Dielectric-constant gas thermometry is being further developed at PTB to measure thermodynamic temperature and the Boltzmann constant k at the triple point of water. Due to the small electric susceptibility of gases, the targeted relative uncertainty of k of the order of 2 ppm can be achieved only if gas pressures up to 7 MPa and special 10 pF capacitors for the susceptibility measurements, including very large multi-ring toroidal cross capacitors, are used. This required development of a huge measuring system having a large heat capacity. Since the temperature measurement must be traceable to the triple point of water at a level of the order of 0.1 mK, a corresponding stability and homogeneity of the thermal conditions has to be realized. The design of the system and data characterizing its thermal parameters is described. The experimental results are compared with estimations based both on simple models and finite-element calculations.

Keywords Boltzmann constant · Primary gas thermometry · Temperature control

1 Introduction

In response to the CIPM proposal to give the Boltzmann constant k a fixed value for a redefinition of the base unit kelvin [1], many projects have been started to measure independently the value of k. Promising methods are dielectric-constant gas thermometry (DCGT) [2,3], acoustic gas thermometry [4,5], and Doppler-broadening thermometry [6,7]. An overview of these methods is given in [8]. Within the framework of the iMERA Joint Research Project "Boltzmann constant" (JRP No. T1.J1.4), PTB designed a new DCGT experimental setup. This decision has been taken in

T. Zandt (✉) · B. Fellmuth · C. Gaiser · A. Kuhn
Physikalisch-Technische Bundesanstalt, Abbestr. 2-12, Berlin 10587, Germany
e-mail: Thorsten.Zandt@ptb.de

view of the excellent experimental DCGT results, which were obtained in the low-temperature range [2,9,10] and allowed the setup of a thermodynamic temperature scale between 3.7 K and 26 K.

DCGT is based on the idea to replace the density in the state equation of a gas by the dielectric constant ε. For an ideal gas, this yields the simple relation between the pressure p and ε: $p = kT(\varepsilon - \varepsilon_0)/\alpha_0$ where ε_0 is the exactly known electric constant and α_0 is the static electric dipole polarizability of a particle. For a real gas, the interaction between the particles has to be considered by combining the virial expansions of the state equation and the Clausius–Mossotti equation [2]. Thus, for determining the DCGT results in the ideal-gas limit, isotherms have to be measured. Then, a polynomial fit to the obtained pressure versus dielectric constant dependence yields also the slope of the linear portion of this dependence near zero pressure describing the ideal-gas behavior. If the polarizability of the measuring gas is known, DCGT is a primary thermometry method, i.e., it allows measurements of both thermodynamic temperature values and, at a known temperature, the Boltzmann constant. The only temperature, which is known by definition, is that of the triple point of water (TPW).

The dielectric constant is determined via the change of the capacitance of a suitable capacitor measured with and without the measuring gas. Helium is the only gas, the polarizability of which can be calculated theoretically with the necessary uncertainty well below one part in 10^6 [11,12]. But the polarizability of helium is very small. To give an example, at a pressure of 0.1 MPa and the TPW, the electric susceptibility of helium has only a value of 7×10^{-5}. As a consequence of this, the design of the DCGT used for the experiments performed at PTB in the low-temperature range loses accuracy due to the decrease of sensitivity at higher temperatures around the TPW. The new DCGT setup, which is being built-up and tested, has the necessary sensitivity because it allows performance of measurements at pressures up to 7 MPa. One main problem of these measurements is the fact that the deformation of the capacitor electrodes under pressure influences significantly the change of the capacitance, i.e., the effective compressibility has to be determined with the necessary small uncertainty. The investigation of systematic error sources requires comparisons of the effective compressibilities of quite different special 10 pF capacitors. For this reason, both cylindrical capacitors and very large multi-ring toroidal cross capacitors have been developed. In view of the dimensions of the capacitors surrounded by rigid pressure vessels, a huge measuring system having a very large heat capacity had to be realized. This system is placed in a vacuum can for thermal isolation. The targeted relative uncertainty of the determination of k at the TPW amounts to about 2 ppm, i.e., the temperature measurement must be traceable to the TPW at a level of the order of a tenth of a mK. This is possible only if in turn the vacuum can is placed into a thermal environment of sufficient quality. For this purpose, a huge liquid-bath thermostat has been designed, produced, and tested that is described in an accompanying article [13]. The thermostat works in the temperature range from the triple point of mercury to the melting point of gallium for checking purposes. It has been already verified that both the instability and the inhomogeneity of the bath temperature are well below 1 mK in the central working volume (diameter 500 mm, height 650 mm), in which the vacuum can containing the measuring system of the DCGT will be placed.

This article is organized as follows. In Sect. 2, the design of the new DCGT measuring system including the capacitors and the pressure vessels is described. Test results characterizing the thermal conditions within the system are presented in Sect. 3. These results concern temperature stability and homogeneity as well as time constants for thermal equilibration that are important for estimating static and dynamic temperature-measurement errors, respectively. In Sect. 4, the experimental data are compared with estimates deduced from both a simple model and finite-element-method (FEM) calculations. Conclusions are drawn and an outlook is given in Sect. 5.

2 Design of the Measuring System

The main parts of the measuring system are a 20 mm thick central copper plate (diameter 430 mm), pressure vessels that are thermally anchored to this plate and contain the measuring capacitors, both made of stainless steel, a 5 mm thick top copper plate, copper rods having a diameter of 40 mm that connect the two plates with each other (distance 400 mm), and a surrounding isothermal shield made of a 5 mm thick copper sheet. Figure 1 shows a photograph of the system without the shield and Fig. 2 illustrates its housing within the measuring chamber consisting of a vacuum can to be inserted into the liquid-bath large-volume thermostat described in [13]. The vacuum can allows realization of vacuum isolation or a defined thermal contact between the measuring system and the can walls via exchange gas. The copper rods run from the system through the top flange of the vacuum can into copper cylinders, which guarantee good thermal contact to the bath liquid (thermal resistance between the solid cylinders and the liquid smaller than $0.02\,\mathrm{K}\cdot\mathrm{W}^{-1}$). If two cylindrical capacitors and two cross capacitors are inserted, the mass of the central plate, the pressure vessels, and the capacitors together (plate assembly) amount to about 100 kg. To achieve acceptable thermal time constants, the thermal resistance between the central plate and the bath should be as small as possible. This is the reason for the large diameter of the copper rods and the use of a relatively thick copper sheet for the shield. The obtained thermal resistances are estimated in Sect. 4. The shield can be tightly screwed to the plates with two loop-type clamps. To enable an investigation of the influence of the thermal resistances, the thermal resistance between the copper rods and the central plate can be adjusted by the aid of fittings made of materials having different thermal conductivities. For improving the thermal contact between solid parts, grease is applied as a contact agent.

The temperature of the measuring system will be controlled using a thermistor as sensor, which is attached to the center of the central plate, and four equal heaters located on the plate near the copper rods. This arrangement should minimize temperature inhomogeneities. But for the test measurements described in this article, one heater was located in the center of the plate and different temperature sensors were attached to the plate and the top ends of the cylindrical capacitor electrodes, respectively (see Fig. 3). The sensors are four industrial platinum-resistance thermometers (IPRTs) and two thermopiles consisting each of ten copper-constantan thermoelements. The reading of the thermopiles gives direct information on the temperature difference between the junctions, i.e., an individual calibration was not necessary. The IPRTs have been

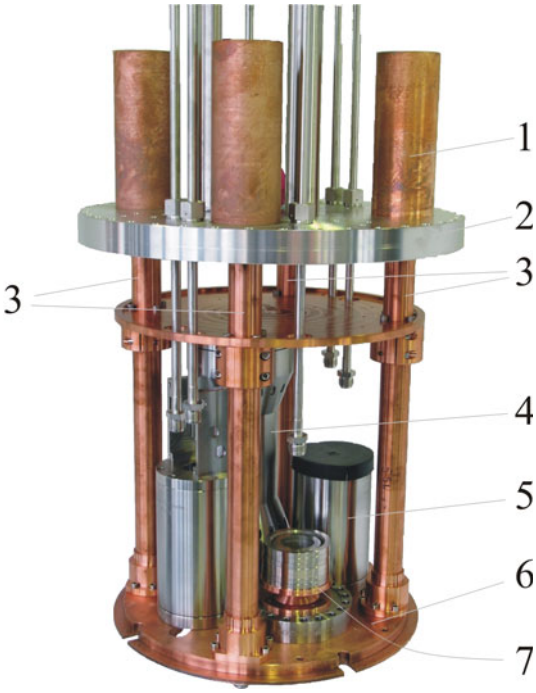

Fig. 1 Photograph of the measuring system without the isothermal shield together with parts of the vacuum can: *1* copper cylinders for improving the thermal contact to the bath; *2* top flange of the vacuum can; *3* copper rods; *4* pressure vessel for cross capacitors with up to 2×25 rings; *5* pressure vessel for a cylindrical capacitor; *6* central copper plate; *7* 2×7 ring toroidal cross capacitor

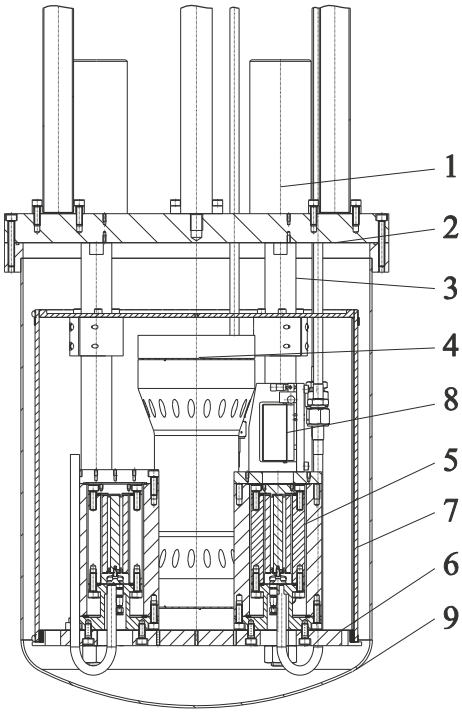

Fig. 2 Design drawing of the measuring system located inside the vacuum can: Numbers *1–6* as in Fig. 1; *7* isothermal copper shield consisting of two parts; *8* mounting for a plane mirror interferometer; *9* vacuum can with its bottom sheet

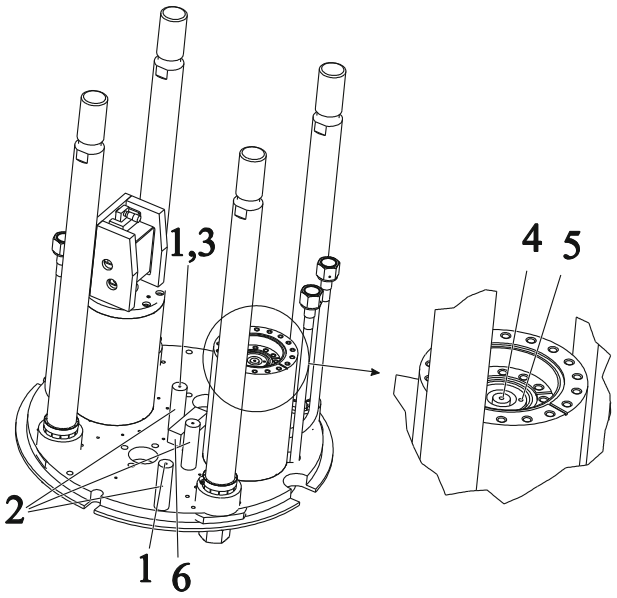

Fig. 3 Configuration of the temperature sensors for the investigation of the thermal parameters of the measuring system containing two cylindrical capacitors: *1* IPRT; *2* thermopile junctions; *3* center of the central copper plate; *4* inner cylindrical electrode; *5* outer electrode, *6* heater

calibrated individually only at the TPW. This was sufficient because they were used only for measuring temperature changes. A good thermal contact between the sensors and the parts of the measuring system was obtained by fitting the IPRTs into holes together with grease as a contact agent and by gluing both the electrical leads of the IPRTs and the thermocouple leads on copper mounting bobbins over lengths of several 100 mm. The localized heating at the center allowed investigations of the magnitude of temperature inhomogeneities during heating as well as the equilibration processes after switching off the heater. This is important for future DCGT experiments because the flow of the measuring gas during changes of the pressure causes warming or cooling localized at the pressure vessel containing the measuring capacitor.

The special 10 pF capacitors, which are being produced and tested at PTB, are shown in Figs. 4 and 5. The new design of the cylindrical capacitors (see also [8]) allows reduction of the influence of the change of the capacitor dimensions under pressure by one order of magnitude when compared with the classical design [2]. For this purpose, a small ground-shield spacer exits between the electrodes both at the bottom and at the top. The effective capacitor length is given by the distance between the two ground-shield spacers. With this design, it is possible to correct for the change of the dimensions based on measuring the deformation of the pressure vessel surrounding the capacitor using a plane mirror interferometer (resolution 0.1 nm). In a second experimental setup, the inner pressure vessel is surrounded by an outer one. A compensation pressure in the outer vessel prevents bending of the bottom and top plates of the inner vessel. Both the setups allow calculations of the effective compressibility of the capacitor if the compressibilities of the construction materials

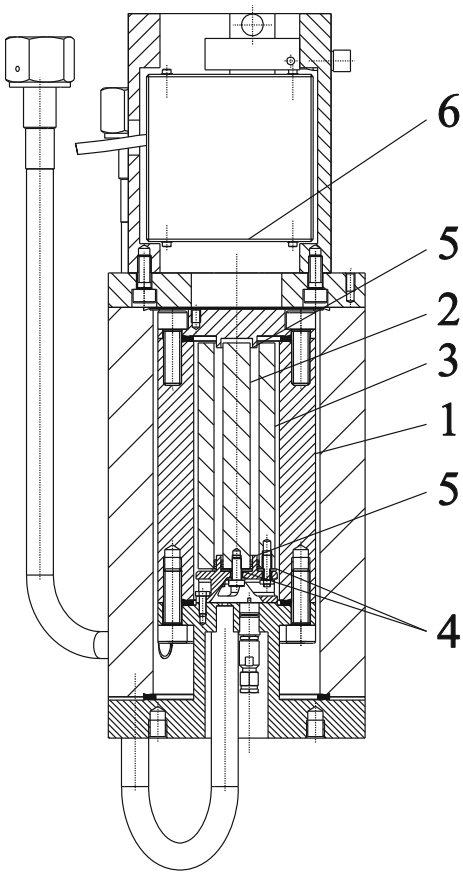

Fig. 4 New design of the cylindrical capacitors: *1* pressure vessel connected with ground; *2* inner electrode (outer diameter of 12 mm, height of 100 mm); *3* outer electrode (inner diameter of 20 mm, height of 100 mm); *4* electrical isolation; *5* cylindrical ground-shield spacer; *6* mounting for a plane mirror interferometer (in an alternative experimental setup, the mounting is replaced by a second, outer pressure vessel surrounding the inner one)

are known individually with the necessary uncertainty from measurements applying resonant ultrasound spectroscopy. For the investigation of systematic error sources, it is necessary to compare the behavior of capacitors of quite different designs. As an alternative to the cylindrical capacitors, therefore, multi-ring toroidal cross capacitors (up to 2×25 rings for 10 pF capacitors) are being also produced and tested. One of the different realized ring shapes is shown in Fig. 5. The advantage of cross capacitors is the fact that distances change under pressure and surface films cause second-order effects, i.e., their effective compressibility is very close to the volume compressibility of the construction materials. But the relatively large dimensions of cross capacitors are disadvantageous. The developed surrounding vessels for pressures up to 7 MPa have a largest diameter of 152 mm and a height of 370 mm. These vessels are the main reason for the large dimensions of the measuring system. The design and parameters of the three-terminal capacitors together with their connection scheme as well as of the bridge will be published in detail elsewhere later in [14]. For this article, on the one hand their dimensions and masses are of interest. On the other hand, it should be emphasized that the capacitors have to be surrounded by pressure vessels

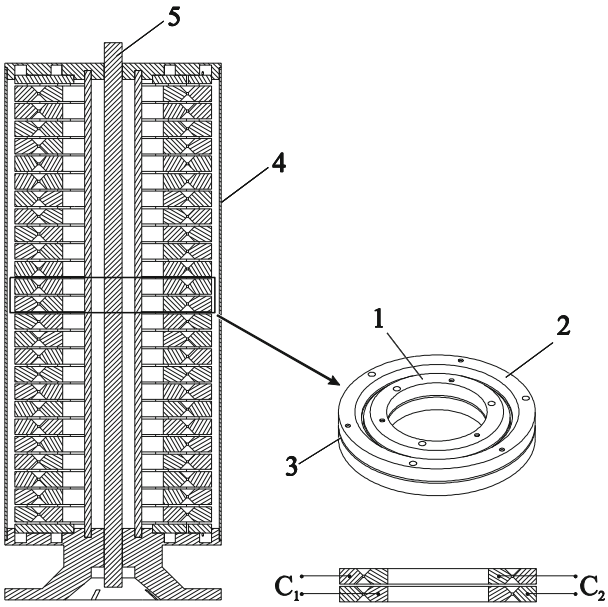

Fig. 5 2 × 25-ring toroidal cross capacitor: a single cross capacitor consists of two inner and two outer rings, see the drawings on the *right*. The cross capacitance is deduced as the weighted mean of the two capacitance values C_1 and C_2 measured each between the inner and the outer rings being diagonally opposite. For obtaining 10 pF, the individual capacitors are connected in parallel. The heights of all rings together with electrical isolation and the outer diameter amount to 209 mm and 69 mm. *1* inner ring (outer diameter of 67 mm, height of 5 mm); *2* outer ring (inner diameter of 69 mm, height of 5 mm); *3* electrical isolation; *4* electrical shield surrounding the whole capacitor; *5* mounting rod

for high-purity measuring gases. It is therefore not possible to measure their temperature directly. This fact makes it necessary to simulate the thermal behavior with FEM calculations, see Sect. 4, using parameters, which have been determined in dedicated preparatory experiments as discussed in Sect. 3.

3 Experimental Investigation of the Thermal Parameters

In this section, experimental results are presented that characterize the thermal conditions inside the new DCGT setup described in Sect. 2. Applying this setup, the temperature of the measuring gas and thus of the capacitor electrodes has to be known traceably to the TPW with an uncertainty at a level of a tenth of a mK. Since the high purity of the measuring gas must be guaranteed, direct temperature measurements inside the pressure vessels surrounding the electrodes are not possible. Therefore, it is essential to determine the thermal parameters of the setup from dedicated preparatory experiments before evaluating the experimental data. During the DCGT experiments, only changes of the capacitance values give information on a drift of the temperature inside the vessels.

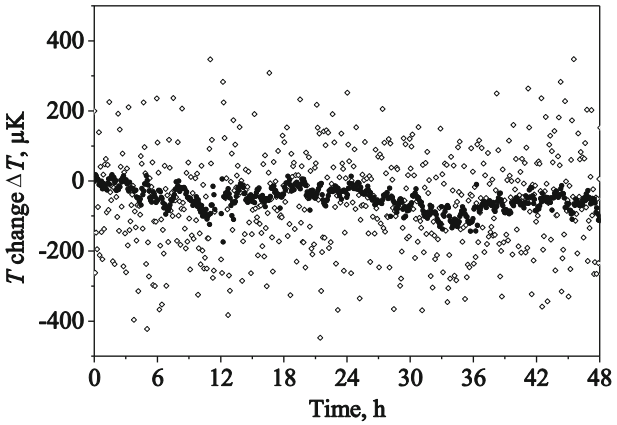

Fig. 6 Temperature readings of two IPRTs versus time over 48 h: *Open diamonds* IPRT in the bath of the thermostat near to the vacuum can surrounding the measuring system; *filled circles*: IPRT attached to the center of the central copper plate of the measuring system. Each data point is the mean of the readings recorded in a 5 min period. In each case, the points give the deviation from the corresponding mean of the first 20 points. No temperature control was used inside the measuring system

The dedicated experiments were performed with the experimental setup documented in Fig. 3. The stability of the temperature at the center of the central copper plate without control is compared with that in the bath of the thermostat close to the vacuum can in Fig. 6 over 48 h. The standard deviations of the temperature values measured at the two positions amount to 0.07 mK (copper plate) and 0.19 mK (bath). This result is impressive. The thermal environment realized with the precision liquid-bath large-volume thermostat has a quality, which leads even without temperature control to the necessary small instability well below 1 mK inside the measuring system. Oscillations of the bath temperature are damped by the large heat capacity of the system. Thus, for measuring isotherms, the main problem is caused by the temperature changes due to warming or cooling during the flow of the measuring gas for changes of the pressure inside the pressure vessels. This warming or cooling is a localized source of a distortion of the temperature field. For investigating the time constants of thermal equilibration processes, such a localized distortion was simulated by heat pulses using the heater attached to the center of the central copper plate. In a first heating experiment, this was done in vacuum, which is the worst case. The upper diagram of Fig. 7 shows the readings of the four IPRTs as a function of time before, during, and after heating in vacuum over 21 min with a power of 28 W. (The results of FEM calculations plotted in the lower diagram for comparison purposes are discussed in Sect. 4.) After switching on the heater, the temperature of the copper plate increases immediately, whereas at the top of the stainless steel cylindrical electrodes, a delay was observed due to the small thermal conductivity of stainless steel ($15\ \mathrm{W \cdot m^{-1} \cdot K^{-1}}$). In the insert, a logarithmic scale is used for the ordinate to get more information on the physics of the processes. In all four cases, the equilibration does not follow a simple exponential law, as is the case only for first-order time-delay elements. This is reasonable because, for instance, for the copper plate, three equilibration processes

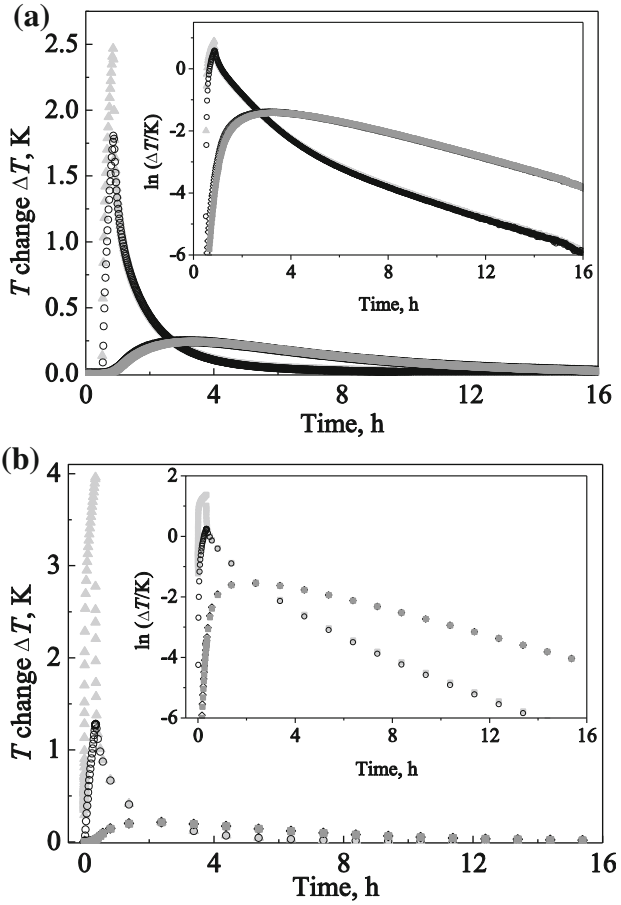

Fig. 7 Temperature readings versus time of four IPRTs located in the measuring system (cf. Fig. 3) at the center (*filled triangles*) and the edge of the central copper plate (*open circles*) as well as at the top of the inner (*filled squares*) and outer capacitor electrodes (*open diamonds*) before, during, and after a heat pulse of 28 W over 21 min at the center of the plate in vacuum. *Upper diagram* (**a**): experimental data points, where each point is the mean of the readings recorded in a 1 min period. In all the four cases, the points give the deviation from the corresponding mean of the first 10 points. The scale of the ordinate is linear for the main diagram and logarithmic for the insert. *Lower diagram* (**b**): FEM calculation results, where in all four cases the calculated points give the deviation from the starting value before the beginning of the heating

are relevant, namely, equilibration within the plate (strictly together with the pressure vessels and the capacitors), within the copper rods and the shield, and between the plate and the bath via the rods and the shield. A fit of a single exponential function to the equilibration curves of the copper plate in the whole period after switching off the heater yields a mean time constant of about 1 h, but the data points are approximated acceptable only with two functions containing time constants of about 0.9 h and 3.3 h. The mean time constant at the top of the electrodes in the period from 5 h to 16 h is essentially larger and amounts to 5.0 h. This large time constant requires optimization of the flow of the measuring gas during pressure changes in order to

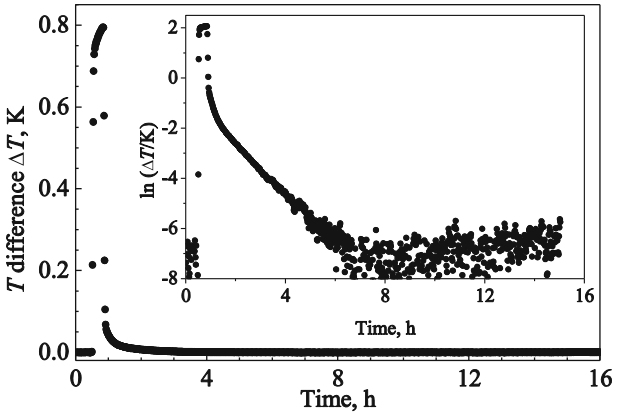

Fig. 8 Temperature reading ΔT of the differential thermopile, the junctions of which are attached to the center and edge of the central copper plate of the measuring system, respectively, (cf. Fig. 3), versus time before, during, and after a heat pulse of 28 W over 21 min at the center of the plate in vacuum. Each data point is the mean of the readings recorded in a 1 min period. All points give deviations from the mean of the first 10 points

minimize the distortion of the temperature field. Fortunately, the results obtained in vacuum are relevant for measuring the zero-pressure capacitance value, for which it is not dangerous to wait long because outgassing cannot influence the results as during the measurement with gas.

Figure 8 gives an impression of the thermal gradients and equilibration processes, mainly within the central copper plate via the temperature reading of the differential thermopile, the junctions of which are attached to the center and the edge of the plate. After switching on the heater, the reading, which gives directly the temperature difference between the center and the edge, increases rapidly over about 5 min, but then the temperature of the edge follows reasonably that of the center. In the insert, the scale for the ordinate is again logarithmic. After switching off the heater, the shown time dependence consists of at least three quasi-linear portions before equilibrium is reached. (The scatter after about 6 h corresponds to a voltage noise of 1 μV, which is the limit of the simple equipment used for the preparatory experiments.) Thus, in accordance with theory [15], even the thermal equilibration within a homogeneous body is not a simple exponential. (A first-order time-delay element, which has a simple exponential response, is only realized if the temperature of a homogeneous body approaches that of a large reservoir via a thermal resistance with its own negligible heat capacity.) The mean time constant of the thermal equilibration within the central copper plate amounts to about 1 h.

To get a feeling for the time constants of the thermal equilibration of the capacitor plates when the thermal conduction through the measuring gas reduces the thermal resistances, a second heating experiment with helium exchange gas at a pressure of 0.1 MPa in the vacuum can was performed. The results obtained are presented in Fig. 9 in a manner analogous to the presentation of the vacuum data in Fig. 7. Fortunately, the mean time constant at the top of the electrodes in the period from 2 h to7 h is now essentially smaller than in the vacuum case and amounts to 1.8 h. (The two time

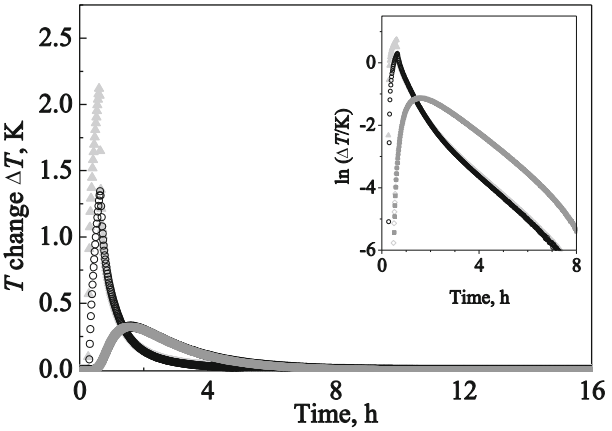

Fig. 9 Temperature readings versus time of four IPRTs located in the measuring system (cf. Fig. 3) before, during, and after a heat pulse of 28 W over 21 min at the center of the central copper plate in helium exchange gas at a pressure of 0.1 MPa. The pattern of the *symbols* is the same as in Fig. 7. Each experimental data point is the mean of the readings recorded in a 1 min period. In all four cases, the points give deviations from the corresponding mean of the first 10 points. The scale of the ordinate is linear for the main diagram and logarithmic for the *inset*

constants resulting for the central copper plate from a description as a second-order time-delay element are also reduced in the helium exchange gas and amount to 0.5 h and 1.6 h, respectively, but this is of minor interest here.) With such a time constant of the capacitor plates, it is possible to measure an isotherm within a few days if the flow of the measuring gas during pressure changes is optimized and thus the distortion of the temperature field is minimized. In view of the high long-term stability of the temperature of the system, which can be expected, see Fig. 6, a measurement period of a few days is acceptable. For the DCGT experiments at the TPW, gas pressures of a few MPa will be used that are much larger than the pressure of the helium exchange gas applied for the second heating experiment. But this will not essentially change the conditions. In the pressure range of interest here, the thermal conductivity of gases depends only weakly on the pressure and an increase of the thermal conduction by convection is unlikely because of the small temperature differences existing in the system during the measurement of an isotherm.

4 Comparison of Experimental Data and Theoretical Estimates

For an understanding of the basic physics of a process, it is helpful to establish a rough model, which is as simple as possible. This can be done for the thermal equilibration process within the measuring system after a heat pulse, discussed in the preceding section, as follows. If the equilibration within the central copper plate together with the pressure vessels and the capacitors (plate assembly) as well as within the copper rods and the shield is neglected, the measuring system can be treated as a first-order time-delay element. The plate assembly is the body, the temperature of which changes with time and which has a heat capacity C, the bath of the thermostat is the large

Table 1 Material properties

Parameters	Copper [16]	Stainless Steel [15] (X2CrNi-MoN17-13-3)	Sapphire [17]
Density ($kg \cdot m^{-3}$)	8900	7980	3980
Thermal conductivity ($W \cdot m^{-1} \cdot K^{-1}$)	398	15	45
Specific heat ($J \cdot kg^{-1} \cdot K^{-1}$)	383	500	718

reservoir acting as a heat sink, and the parallel connection of the copper rods and the shield can be described by a thermal resistance R limiting the heat flow. For a first-order time-delay element, the RC model is valid, i.e., the time constant τ is equal to the product RC. The estimation of RC has been performed using the following parameters (cf. Table 1): thermal conductivity of copper: $398\ W \cdot m^{-1} \cdot K^{-1}$; thermal conductivity of helium at a pressure of 0.1 MPa (280 K): $0.1485\ W \cdot m^{-1} \cdot K^{-1}$ [15]; specific heat of steel: $500\ J \cdot kg^{-1} \cdot K^{-1}$ (the specific heat of copper is slightly smaller, but this is not important for estimating the order of magnitude of the effects). The resulting thermal resistance of the copper rods and the copper shield connected in parallel amounts to about $R_{Cu} = 0.11\ K \cdot W^{-1}$. With the mass of the plate assembly during the heating experiments of 77 kg (only the cylindrical capacitors and their pressure vessels were placed into the system), which corresponds to a heat capacity of about $C = 39\ kJ \cdot K^{-1}$, the time constant is estimated to be $\tau_{Cu} = 1.2$ h. If helium exchange gas is provided in the vacuum can at a pressure of 0.1 MPa, the overall thermal resistance between the bath of the thermostat and the plate assembly is reduced to $R_{Cu+He} = 0.08\ K \cdot W^{-1}$ and thus the time constant to $\tau_{Cu+He} = 0.8$ h. These time-constant estimates are comparable with the smaller experimental values, i.e., the RC model describes for one part of the thermal equilibration process the order of magnitude of the effects correctly. The other parts cannot be treated, in principle, with this simple model.

Though the simple RC model yields the correct order of magnitude for the time constant of the first part of the thermal equilibration of the plate assembly after heating, FEM calculations were performed to investigate the processes in detail. This is especially necessary for a description of the temperature versus time dependence of the capacitor electrodes. The commercial software applied for the calculations was ANSYS Multiphysics[1] (version 11.0SP1).

Using the geometry described in Fig. 2, a model was generated with ANSYS DesignModeler (see footnote 1). The model was then map-meshed with ANSYS Workbench (see footnote 1). The values of the material properties used are given in Table 1. (In the small temperature range of interest here, their temperature dependence has been neglected.) Two types of thermal boundary conditions were applied to the FEM as follows: (1) convection of the water around the vacuum can, the top flange of the vacuum can and the copper cylinders, which are arranged on the top flange,

[1] Identification of commercial equipment and materials in this article does not imply recommendation or endorsement by the PTB, or does it imply that the equipment and materials identified are necessarily the best available for the purpose.

yields a heat transfer coefficient of 1200 $W \cdot m^{-2} \cdot K^{-1}$ at 5.8 °C. (2) Convection of the ambient air around the upper tubes yields 2 $W \cdot m^{-2} \cdot K^{-1}$ at 21.5 °C. The simulation was started with a steady-state thermal analysis. The result of this was used as an initial condition for transient thermal analysis. As an additional boundary condition, a heat flow was used for the simulation of the experimental heat pulse (power of 28 W, time period of 21 min).

First results of the FEM calculations are illustrated in the lower diagram of Fig. 7 and can be compared directly with the experimental data obtained in vacuum. This comparison shows that the theoretically estimated behavior is basically similar to the experimentally observed one. (The temperature values, which have been calculated for the IPRT located at the center of the central copper plate, are excessively increased during and shortly after the heat pulse. This result is an artifact of the model used, which neglects the thermal resistance between this IPRT and the heater. But this is not an obstacle for the discussion of the general equilibration behavior of interest here.) An evaluation of the calculation results as done for the experimental ones has yielded the following values for the time constants of the vacuum experiment: plate assembly: 0.6 h and 2.0 h, capacitor electrodes: 5.4 h. Thus, the order of magnitude of the experimentally found time constants can be described correctly by the theoretical calculations. It is worthwhile to note that the large time constants of the capacitor electrodes in the vacuum case have been calculated without assuming thermal contact resistances between the different solid parts of the system. The achieved agreement between experiment and theory will allow estimates of the dynamic temperature-measurement errors during the planned DCGT experiments with a sufficiently small uncertainty since the calculations will be accompanied by a careful observation of the drift of the capacitance values with time. Furthermore, the quality of the calculation estimates will be improved by adjusting the input parameters considering experimental data. Calculations to simulate the results of the exchange-gas experiment are being done. They are more complicated because it is also necessary to deal with the heat transfer between the gas and the solid parts that introduces additional, badly known parameters.

5 Conclusions

A new experimental setup for DCGT at temperatures around the TPW is being designed, built, and tested at PTB. The results concerning the thermal conditions in the measuring system, which contains special capacitors as the sensors of the DCGT, presented in the article allow three main conclusions to be drawn:

- The stability and homogeneity of the temperature of the central copper plate, which is the thermal reference for all necessary high-precision sensors, will allow performance of temperature measurements traceable to the TPW as accurate as necessary for the determination of the Boltzmann constant at the TPW with the targeted relative uncertainty of the order of 2 ppm. The uncertainty component due to static temperature-measurement errors can be decreased below one tenth of a mK.
- The time constants of the thermal equilibration processes will allow measurements of a DCGT isotherm within a few days, which is acceptable in view of the stability

of the system. But this requires minimization of the distortion of the temperature field inside the measuring system by optimizing the flow of the gas during pressure changes.
- The equilibration processes can be simulated by FEM calculations with a quality, which is sufficient for decreasing also the uncertainty of the estimates for dynamic temperature-measurement errors below one tenth of a mK. This will be possible because the theoretical estimates will be accompanied by careful observation of the drift of the capacitance values with time.

Further development of the new DCGT setup is challenging since the following problems have to be solved:

- *Investigation of outgassing*: The outgassing from the walls inside the pressure vessel containing the measuring capacitor during the measurement of a DCGT isotherm causes contamination of the gas. Since the atoms of the measuring gas and of impurities such as hydrogen have very different polarizabilities, the gas must be very pure, e.g., helium at a level of 99.99999 %. The outgassing may, therefore, set an upper limit for the time period, in which the measurements can take place, because in this period the impurities cannot be removed.
- *Control of the temperature of the central copper plate*: The temperature control is complicated because warming and cooling are very asymmetric. The temperature can be quickly increased by heating, but it declines only slowly by thermal conduction. This may require optimization of the thermal resistances and the addition of Peltier cooling.
- *Improvement of the FEM calculations*: The necessary improvements concern primarily the simulation of the thermal behavior of the large multi-ring toroidal cross capacitors inside the pressure vessels. The design of these cross capacitors is much more complicated than that of the cylindrical capacitors, and the large number of thermal contact resistances may be problematic. The simulation of the behavior of cylindrical capacitors should also be improved by including an exchange gas and adjusting the input parameters considering data obtained in dedicated preparatory experiments.
- *Optimization of the gas flow*: The flow of the measuring gas for changing the pressure requires pumping or compression resulting in a decrease or increase of the temperature. The optimization of this process is directed to minimize the distortion of the temperature field inside the measuring system. It requires performing thermodynamic calculations, which should yield information on the optimum rate of gas flow and pre-cooling.
- *Application of pressure balances*: Gas pressures up to 7 MPa can be measured with a relative uncertainty of a few ppm only with the aid of pressure balances. But these devices do not allow continuous measurements because of the loss of gas through the clearance between the piston and cylinder, by which the piston moves slowly down. At the desired uncertainty level, the gas can only be fed cyclically, interrupting the measurement. The cycling has to be made such that the possible additional gas flow, e.g., due to the handling of valves, does not disturb the temperature field inside the measuring system.

Acknowledgment The research within the EURAMET joint research project receives funding from the European Community's Seventh Framework Programme, iMERAPlus, under Grant Agreement No. 217257 which is gratefully acknowledged.

References

1. Recommendation T2 (2005) to the CIPM: New Determinations of Thermodynamic Temperature and the Boltzmann Constant, Working Documents of the 23rd Meeting of the Consultative Committee for Thermometry (BIPM, Document CCT/05-31, 2005)
2. H. Luther, K. Grohmann, B. Fellmuth, Metrologia **33**, 341 (1996)
3. B. Fellmuth, J. Fischer, C. Gaiser, N. Haft, in *Proceedings of TEMPMEKO 2004, 9th International Symposium on Temperature and Thermal Measurements in Industry and Science*, vol. 2, ed. by D. Zvizdić, L.G. Bermanec, T. Stašiić, T. Veliki (LPM/FSB, Zagreb, Croatia, 2005), pp. 73–78
4. R.M. Gavioso, P.A. Giuliano Albo, G. Benedetto, R. Spagnolo, *Proceedings of CPEM 2006* (CPEM, Turin, Heidelberg, 1998), pp. 26–27
5. M.R. Moldover, J.P.M. Trusler, T.J. Edwards, J.B. Mehl, R.S. Davis, Phys. Rev. Lett. **60**, 249 (1988)
6. C. Daussy, M. Guinet, A. Amy-Klein, K. Djerroud, Y. Hermier, S. Briaudeau, Ch.J. Bordé, C. Chardonnet, Phys. Rev. Lett. **98**, 250801 (2007)
7. G. Casa, A. Castrillo, G. Galzerano, R. Wehr, A. Merlone, D. Serafino, P. Laporta, L. Gianfrani, Phys. Rev. Lett. **100**, 200801 (2008)
8. B. Fellmuth, Ch. Gaiser, J. Fischer, Meas. Sci. Technol. **17**, R145 (2006)
9. Ch. Gaiser, B. Fellmuth, N. Haft, Int. J. Thermophys. **29**, 287 (2008)
10. Ch. Gaiser, B. Fellmuth, Metrologia **46**, 525 (2009)
11. W. Cencek, K. Szalewicz, B. Jeziorski, Phys. Rev. Lett. **86**, 5675 (2001)
12. G. Lach, B. Jeziorski, K. Szalewicz, Phys. Rev. Lett. **92**, 233001 (2004)
13. A. Merlone, F. Moro, T. Zandt, C. Gaiser, B. Fellmuth, Int. J. Thermophys. doi:10.1007/s10765-010-0708-x
14. T. Zandt, C. Gaiser, B. Fellmuth (to be published)
15. H.D. Baehr, K. Stephan, *Heat and Mass Transfer* (Springer, Berlin, Heidelberg, 1998)
16. ASM, *Metals Handbook*, vol. 2 (ASM Handbook Committee, American Society for Metals, Materials Park, OH, 1990)
17. D.G. Archer, J. Phys. Chem. Ref. Data **22**, 1441 (1993)